IX International Conference on Computational Methods for Coupled Problems in Science and Engineering
COUPLED PROBLEMS 2021
E. Oñate, M. Papadrakakis and B. Schrefler (Eds)

TOPOLOGY OPTIMIZATION FOR MANUFACTURABLE THERMOELASTIC METAMATERIALS WITH TAILORED UNIDIRECTIONAL THERMAL EXPANSION

M.J.F. van den Ouden, S. Koppen and M. Langelaar

Department of Precision and Microsystems Engineering
Delft University of Technology
Mekelweg 2, 2628 CD Delft, The Netherlands
e-mail: m.j.f.vandenouden@student.tudelft.nl, s.koppen@tudelft.nl, m.langelaar@tudelft.nl,
web page: https://www.tudelft.nl/

Key words: Thermoelastic Metamaterials, Topology Optimization, Static Condensation, Robust Design, Multi-Material Additive Manufacturing

Abstract. The concept of thermoelastic metamaterials has been around for over two decades. Nevertheless they are rarely applied, due to their poor manufacturability. To enhance their applicability, a topology optimization framework is proposed and verified, able to generate finite thermoelastic unit cell arrays with tailored unidirectional thermal expansion, manufacturable through automated multi-material additive manufacturing methods.

A thermoelastic unit cell array is optimized for near zero thermal expansion. A sample has been fabricated using a low-tech production process, inspired by a multi-material ultrasonic additive manufacturing process, with a unidirectional thermal expansion of $(-4 \pm 8)\,\mu\text{m}/(\text{m}^\circ\text{C})$. With this sample, the numerical predictions have been validated experimentally, confirming the capability of the proposed design approach to generate performant and realizable thermoelastic metamaterials.

1 INTRODUCTION

Thermoelastic metamaterials are composites designed for a tailored or unconventional Coefficient of Thermal Expansion (CTE). They are typically composed of multiple conventional materials with different but positive CTE, which are arranged in a specific periodic microstructure. Upon heating, the difference in CTE of the used materials causes the metamaterial structure to deform, allowing for extremal CTE.

Applications of thermoelastic metamaterials are plentiful. Negative Thermal Expansion (NTE) metamaterials can for example be used in thermally operated fasteners. The volume contraction upon heating allows for easy insertion of the fastener into tight holes

[9]. Zero Thermal Expansion (ZTE) metamaterials can furthermore be used in optical components and precision instruments [13], where high precision and stability under varying thermal conditions is to be achieved. Large Positive Thermal Expansion (PTE) metamaterials are applicable to medical vessel dilators, which should dilate blood vessels when the human body temperature is increasing [10].

One of the most powerful methods to design thermoelastic metamaterials is Topology Optimization (TO). Thermoelastic metamaterials have already been designed using TO [1, 3, 5, 9, 10, 11], in which their effective material properties are determined using the homogenization theory [2], which assumes infinitely repeating unit cells. Thermoelastic unit cell arrays composed of only a small number of unit cells are however manufactured [6, 8, 10, 11]. Since only arrays with a finite number of unit cells can be manufactured, a difference between numerical and physical performance arises in this approach. Optimized designs in literature are furthermore extensively post-processed, to enhance their manufacturability. Thin hinges are for example strengthened and complex shapes are simplified, which compromises their optimality and alters their behaviour. In this paper, we present a new approach to address these disadvantages.

Regarding manufacturability, a combination of the automated methods Ultrasonic Additive Manufacturing (UAM) and Electronic Discharge Machining (EDM) allows metallic thermoelastic metamaterials to be manufactured successfully at useful scales [7]. Only thermoelastic metamaterials with alternating uniform materials layers, each composed of just a single material and locations without material, are manufacturable using this production process. This constraint is considered in this study.

This paper proposes and verifies a TO framework, able to generate finite thermoelastic metamaterials with tailored unidirectional thermal expansion composed of uniform material layers, manufacturable through automated multi-material Additive Manufacturing (AM) methods. A computationally efficient exact Reduced Order Model (ROM), obtained using static condensation [4], is used to determine the thermoelastic response of unit cell arrays with a finite number of unit cells. Comparison of the conventional homogenization theory with this finite unit cell array modelling approach, verifies the inaccuracy of the homogenization theory for the modelling of finite unit cell arrays. Furthermore, minimum length scale control and robustness are established, using a robust optimization formulation [12]. Before describing the framework in further detail, the considered problem is introduced in the next section.

2 OPTIMIZATION PROBLEM

2.1 Design domain

The design domain visualized in Figure 1 is used in an example case considered using the new TO framework. A unit cell is patterned periodically in a finite unit cell array and solid mounting strips are attached to the top and bottom of the structure. Furthermore, consistent with UAM, uniform material layers are enforced in the design domain.

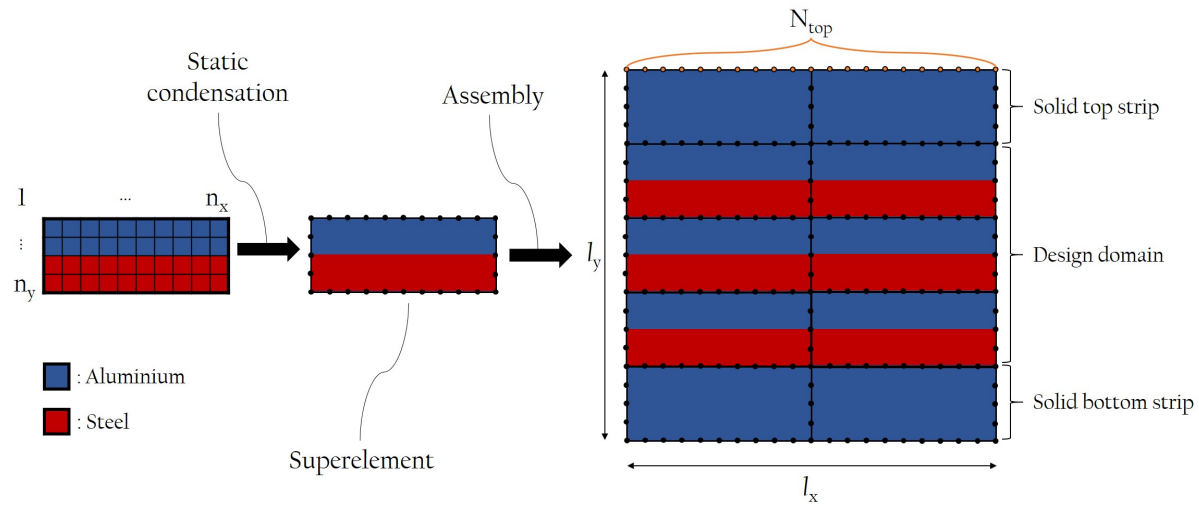

Figure 1: Visual representation of the optimization case and of the procedure to obtain an exact ROM. A 2×3 unit cell array with solid strips is optimized. Dimensions l_x and l_y are equal to 0.15 m $\times$ 0.15 m and each superelement is discretized using $n_x \times n_y$ square finite elements with $n_x = 150$ and $n_y = 60$.

2.2 Formulation

Following the robust approach [12], the worst case of an eroded, intermediate and dilated topology is optimized, to obtain a manufacturing tolerant design. As performance parameter, the compliance of the eroded periodic unit cell array is minimized, for a unit tensile load applied to its top boundary. The unidirectional thermal expansion of the unit cell array is furthermore tailored, by constraining the Mean Square Error (MSE) of the vertical displacement of the top boundary resulting from a unit temperature increase. Volume constraints are enforced on the dilated topology, to constrain the weight of the structure and a lower bound for the element densities is enforced, to prevent singularities of the stiffness matrix. Vertical line symmetry furthermore reduces the size of the design variable vector. The optimization problem is given by:

$$
\begin{aligned}
\min_{\mathbf{x}_1} : \quad & \mathbf{f}^{\{\mathrm{e}\}} \cdot \mathbf{u}^{\{\mathrm{e}\}}, \\
\text{s.t.} : \quad & {g_{\mathrm{MSE}}}^{\{h\}} \leq 0 \qquad \text{for all} \qquad h = \{\mathrm{e}, \mathrm{i}, \mathrm{d}\}, \\
& V_{\mathrm{Aluminium}}^{\{\mathrm{d}\}} \leq V_{\mathrm{Aluminium}}^{*}, \\
& V_{\mathrm{Steel}}^{\{\mathrm{d}\}} \leq V_{\mathrm{steel}}^{*}, \\
& \mathbf{0} \leq \mathbf{x}_1^{\min} \leq \mathbf{x}_1 \leq \mathbf{1}, \\
& \text{Vertical line symmetry}, \qquad (1)
\end{aligned}
$$

in which $\mathbf{x}_1$ is the design vector containing the densities for the elements describing a single unit cell. $\mathbf{f}^{\{\mathrm{e}\}}$ and $\mathbf{u}^{\{\mathrm{e}\}}$ are the nodal force vector and displacement vector for the eroded topology, resulting from the unit tensile load. $V^{\{\mathrm{d}\}}$ and V^* are the volume fractions of the

dilated topology and the user defined upper bound for the volume fractions, respectively. The vector $\mathbf{x}_1^{\min}$ contains the lower bounds for the element densities. g_{MSE} describes the MSE constraint, which is applied on the eroded, intermediate and dilated topologies:

$$g_{\text{MSE}} = \log_{10}\left(\sum_{N_{\text{top}}}(u_{\text{y}} - u_0)^2\right) - \log_{10}\left(c_{\text{MSE}}\right) \leq 0, \tag{2}$$

in which u_{y} is the vertical thermal displacement, for the set of nodes N_{top} on the top boundary of the unit cell array (see Figure 1), resulting from a unit temperature increase. u_0 is the desired vertical thermal displacement for the top nodes, which can be chosen for a specific unidirectional thermal expansion. c_{MSE} describes the upper bound for the defined MSE and controls the allowed variation of the vertical thermal displacement along the top boundary of the unit cell array. A logarithmic transformation is applied, to prevent small sensitivities which could cause numerical problems.

The bounds for the imposed constraints and the desired minimum length scale are provided in Table 1. The minimum length scale is chosen conservatively based on the low-tech production process used for the demonstrator. c_{MSE} is chosen such, that the considered MSE is smaller than one tenth of the MSE expected for a solid steel block of similar size, computed using a zero target vertical thermal displacement. The example case is initialized using uniform density fields, with initial element densities x_0 of 0.25 and 0.75.

Table 1: Constraint bounds and minimum length scale.

Parameter	Value	Description
b	2	Desired minimum length scale in millimeters
c_{MSE}	2.43×10^{-10}	Upper bound MSE constraint in meters squared
$V^*_{\text{Aluminium}}$	0.40	Maximum volume fraction aluminium phase
V^*_{Steel}	0.25	Maximum volume fraction steel phase

3 TOPOLOGY OPTIMIZATION FOR MANUFACTURABILITY

3.1 Reduced order model

An exact ROM is used for the analysis of the finite unit cell arrays, given the geometric similarity of the unit cells, in order to raise computational efficiency. The procedure used to obtain an exact ROM, is visualized in Figure 1. First, the DOFs of a single unit cell are divided in a set of retained DOFs, located at the boundary of the unit cell and a set of condensed DOFs, located at the interior of the unit cell. Static condensation [4] is utilized, to condense the classical Finite Element (FE) equation, such that it is only solved for the set of retained DOFs at the boundary of the unit cell:

$$\left(\mathbf{K}_{\text{rr}} - \mathbf{K}_{\text{rc}}\mathbf{K}_{\text{cc}}^{-1}\mathbf{K}_{\text{cr}}\right)\mathbf{u}_{\text{r}} = \mathbf{f}_{\text{r}} - \mathbf{K}_{\text{rc}}\mathbf{K}_{\text{cc}}^{-1}\mathbf{f}_{\text{c}}, \tag{3}$$

in which the subscripts r and c refer to the set of retained and condensed DOFs, respectively. A superelement is obtained, with a reduced stiffness matrix and force vector, describing the exact behaviour of the unit cell. The superelements are assembled, such that a reduced system of equations is obtained for the finite unit cell array, which is much smaller than the system of equations obtained for a full FEA.

Solid strips adjacent to the thermoelastic unit cell array are included in the ROM. A superelement representing a section of solid strip is generated in a similar fashion, which only has to be done once since the topology of the solid strips does not change during optimization.

3.2 Robust formulation and filter domain extension approach

In the robust formulation [12], the worst case of an eroded, intermediate and dilated topology is optimized. The topologies are obtained by applying a smooth threshold projection to the filtered density field for different threshold values, as visualized in Figure 2.

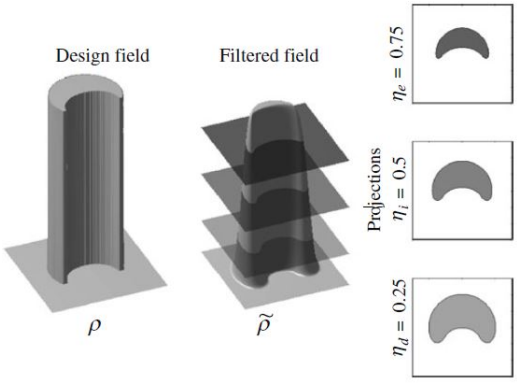

Figure 2: Illustration of the threshold projections for different choices of the threshold value η [12].

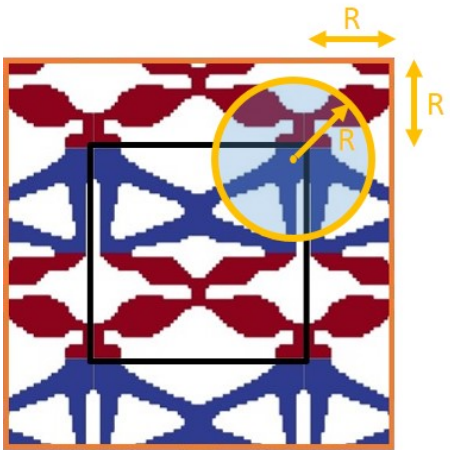

Figure 3: Original filter domain (black) and extended filter domain (orange), for a filter with radius R.

A specific minimum length scale can be established at the interior of an optimized domain, by selecting a specific combination of the used filter radius and threshold values, for a sufficiently sharp threshold projection [12]. Furthermore, the resulting design will be less sensitive to manufacturing inaccuracies, which is desirable for the considered metamaterial. In the new TO framework, the robust formulation is applied to the topology of a single unit cell. The filter boundaries are extended with at least the filter radius, assuming that the considered unit cell is surrounded by identical unit cells as is visualized in Figure 3. Minimum length scale control at the boundary of the unit cells is obtained using the extension, when the filter domain extension is valid and other unit cells indeed adjoin the unit cell boundary.

4 NUMERICAL RESULTS

The topologies of a single unit cell for two cases are given in Figure 5. It can be seen that the topologies for the eroded, intermediate and dilated designs are the same for the case initialized using $x_0 = 0.25$, whilst they vary locally near the corners of the unit cell for the case initialized using $x_0 = 0.75$. The applied robust optimization formulation requires these topologies to be the same. Therefore, void regions smaller than the minimum length scale specified are observed for the intermediate topology of the design initialized using $x_0 = 0.75$, at the locations were the topologies vary locally.

The blueprints for the optimized unit cell arrays, are visualized in Figure 6. Apart from the small void regions observed for the topology initialized using $x_0 = 0.75$, minimum length scale control is successfully obtained for the interior of the unit cell arrays. For boundaries where the used filter domain extension is not valid, so where the unit cells do not connect to other unit cells, minimum length scale control is not obtained as is expected. The void at the top boundary of the top layers of unit cells for example, which adjoins the solid mounting strip instead of a unit cell, is smaller than the specified minimum length scale, since the used filter domain extension is not valid for this boundary. The vertical thermal displacement of the top boundaries of the optimized unit cell arrays are given in Figure 4. For both cases, the vertical thermal displacement of the top boundary of the unit cell array is well below the thermal expansion expected for steel, which is the material of the unit cell arrays with the lowest CTE.

Despite the small void regions observed at its interior, the design initialized using $x_0 = 0.75$ will be analyzed for the purpose of experimental verification. For the design initialized using $x_0 = 0.25$, the contact surface between the material layers is small and a reliable adhesive connection might not be established, which is required for the used low-tech manufacturing method, inspired by a UAM production process [7].

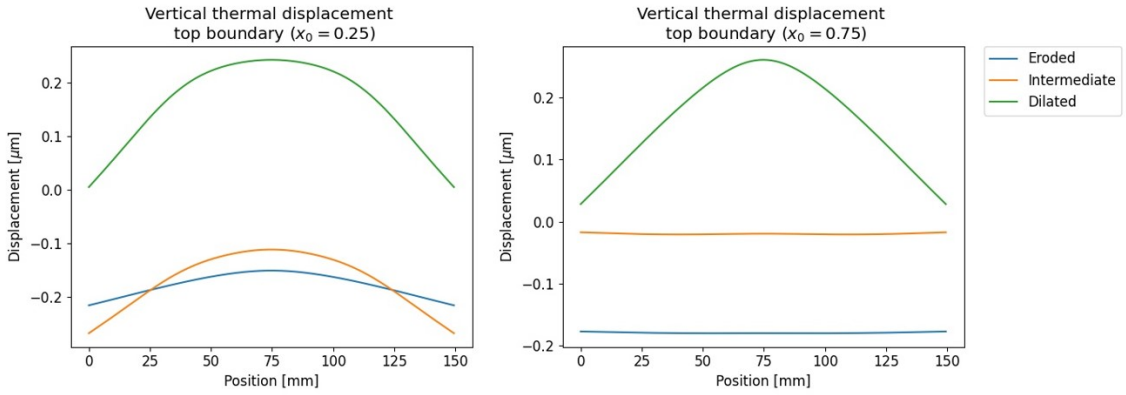

Figure 4: Vertical thermal displacements of the top boundary of the eroded, intermediate and dilated unit cell arrays, for a unit thermal load.

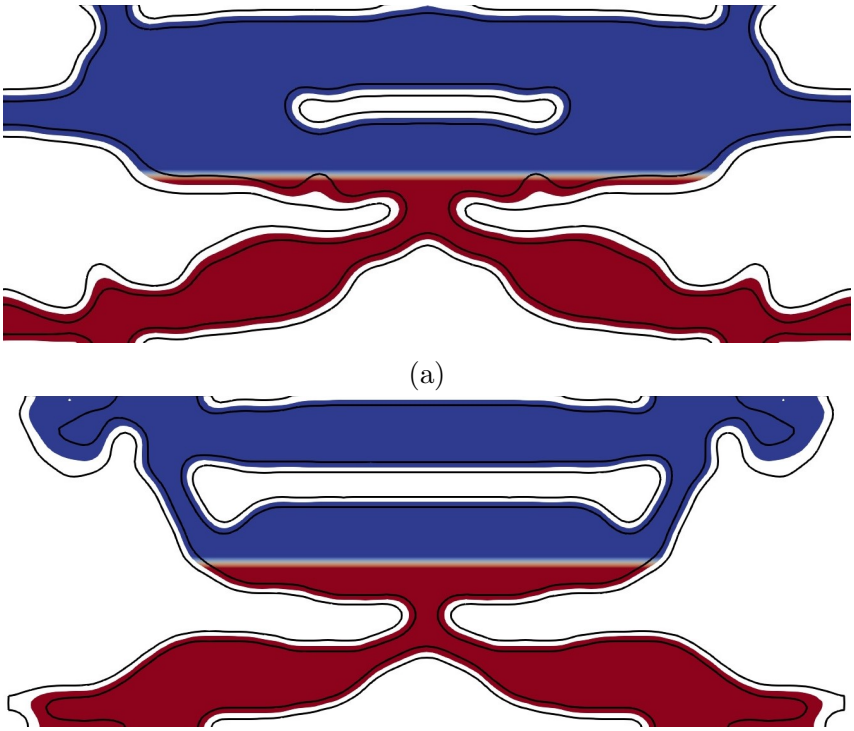

(a)

(b)

Figure 5: Optimized intermediate topology for a single unit cell and contours for the eroded and dilated unit cells, for $x_0 = 0.25$ (a) and $x_0 = 0.75$ (b), composed of aluminium (blue) and steel (red).

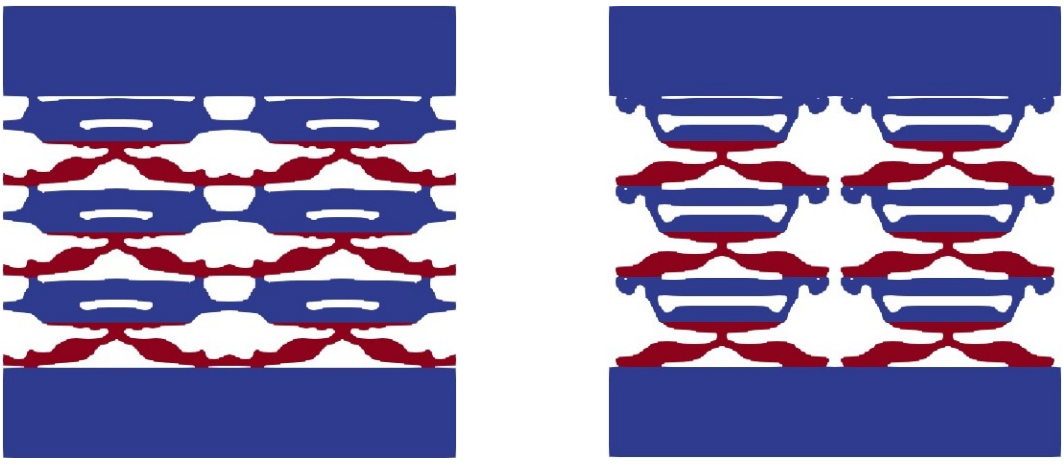

(a) (b)

Figure 6: Optimized intermediate unit cell array topologies, to be used as bluepints for the optimized design, initialized using $x_0 = 0.25$ (a) and $x_0 = 0.75$ (b), composed of aluminium (blue) and steel (red).

5 EFFECT OF ARRAY SIZE

It is of interest to determine the accuracy of the conventional homogenization approach for metamaterial design to the finite cell array modeling applied here. The vertical thermal displacement of the optimized unit cell array initialized using $x_0 = 0.75$, computed using both an exact ROM and the homogenization theory, is considered. Using the homogenization theory, the effective material properties are computed for the unit cell design, assuming an infinite array. The response of the studied finite unit cell array including solid strips is computed using a full FEA, in which the unit cells are modelled using a solid material having the computed homogenized properties. For the exact ROM, the number of unit cells of the array between the solid strips is increased, whilst maintaining the same overall dimensions for the unit cell array. The results are presented in Figure 7.

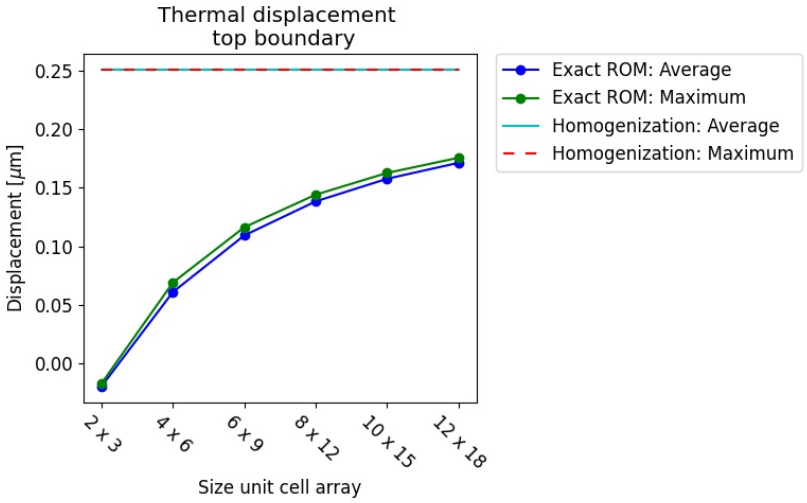

Figure 7: Average and maximum vertical thermal displacement of the top boundary of the unit cell array, computed using the homogenization theory and the exact ROM. Unit cell array size refers to the number of periodically repeated unit cells, so excluding the solid strips.

The vertical thermal displacement for an array size of 2×3 unit cells, used in the optimization case, is considerably lower for the exact ROM than for the homogenization method. Extrapolation of the maximum displacements computed using the ROM, shows that only for array sizes larger than 120×180, the difference in the obtained displacement values for both methods is smaller than 5 %.

The homogenization theory is often used in existing TO frameworks for thermoelastic metamaterials. Small thermoelastic unit cell arrays are however most often manufactured, since the fabrication of large unit cell arrays remains difficult. The exact ROM accounts for the size of the unit cell array and gives a significantly different and more realistic thermoelastic response for small unit cell arrays, compared to the commonly used homogenization theory, whilst preserving acceptable computational costs.

6 EXPERIMENTAL VALIDATION

The unidirectional thermal expansion of the optimized unit cell array initialized using $x_0 = 0.75$, visualized in Figure 4, is well below the thermal expansion expected for steel, which is the material of the optimized unit cell array with the lowest CTE. A detailed 3D FEA of the post-processed design, in which adhesive bonds were modelled between the material layers, confirms this conclusion. Experimental validation is used to confirm that the physical behaviour of the optimized design is in line with the numerical predictions.

6.1 Fabrication

A sample of the optimized design has been fabricated using a low-tech production process, inspired by the UAM production process presented by Parsons [7]. Square bars of aluminium and steel are bonded using Araldite ® 2019 adhesive, which is cured for 1 hour at 130 °C. Subsequently, waterjet cutting is performed with an OMAX MicroMax® to cut the optimized topology from the layered multi-material solid block.

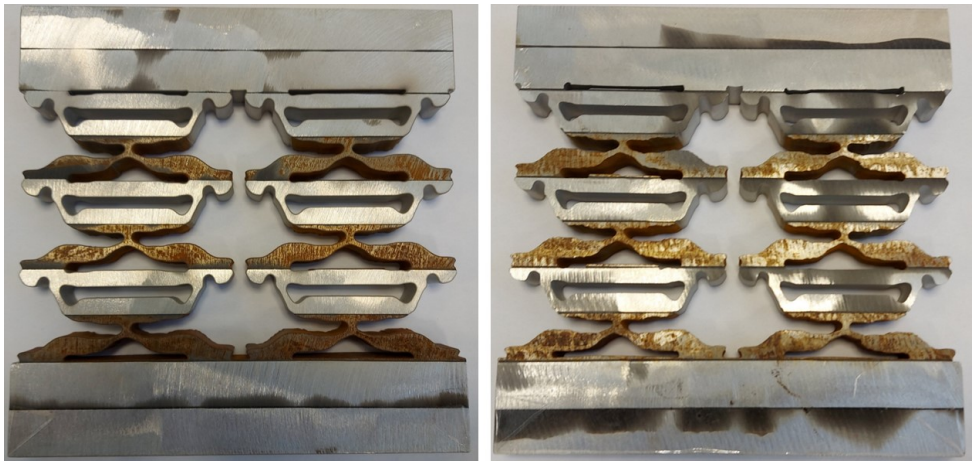

Figure 8: Front (left) and rear (right) view of the manufactured thermoelastic metamaterial structure.

6.2 Measurements

The unidirectional thermal expansion of the optimized sample is determined using the setup schematically visualized in Figure 9. Hot water is poured into the container, which cools down slowly from 40 °C till 30 °C during the measurement. The gap between the measurement frame and both samples is measured using non-contact fiber optic sensors. The unidirectional thermal expansion of the optimized sample can be determined quantitatively, since the CTE of the steel sample is known. The unidirectional thermal expansion is compensated for the sections of the samples protruding above the water, which are possibly not fully subjected to the imposed temperature change.

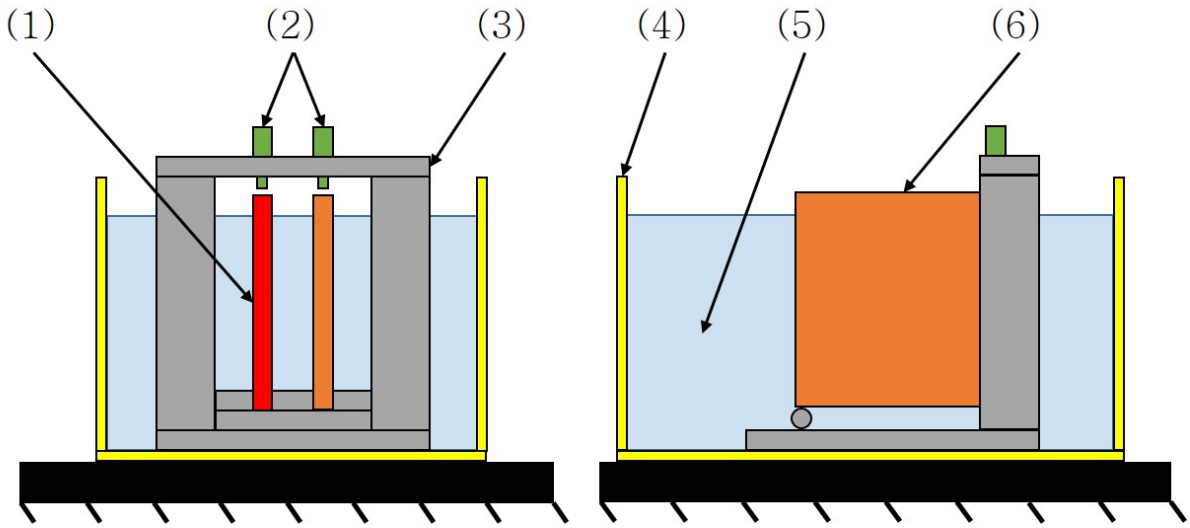

Figure 9: Schematic overview of the experimental setup used to determine the unidirectional thermal expansion of the optimized sample. (1) Optimized sample; (2) Fiber optic sensor heads; (3) Custom made aluminium measurement frame; (4) Container; (5) Water; (6) Steel sample.

6.3 Results

The change in the sensor gaps for the final measurement points of four different measurements are presented in Table 2. The lower the unidirectional thermal expansion of the sample, the larger the shrinkage of the sensor gap due to the shrinkage of the aluminium measurement frame. The shrinkage of the sensor gap for the optimized sample is significantly larger than for the steel reference sample. The unidirectional thermal expansion of the optimized sample is therefore lower than the unidirectional thermal expansion of steel, which is the constituent of the optimized sample with the lowest CTE. An unidirectional thermal expansion of $(-4 \pm 8)\,\mu\text{m}/(\text{m}^\circ\text{C})$ is determined for the optimized sample.

Table 2: Measured change and difference for the sensor gaps of the optimized and steel sample, in which positive values indicate an increase of the sensor gap.

Measurement	$\Delta_{\text{gap,opt}}$ [m]	$\Delta_{\text{gap,steel}}$ [m]	$\Delta_{\text{gap,opt}} - \Delta_{\text{gap,steel}}$ [m]
1	-34.2×10^{-6}	-9.0×10^{-6}	-25.2×10^{-6}
2	-35.0×10^{-6}	-9.2×10^{-6}	-25.8×10^{-6}
3	-31.7×10^{-6}	-6.8×10^{-6}	-24.9×10^{-6}
4	-34.0×10^{-6}	-5.0×10^{-6}	-29.0×10^{-6}

7 CONCLUSIONS

A TO framework for finite thermoelastic metamaterials with tailored unidirectional thermal expansion, manufacturable through automated multi-material AM methods, has been developed and validated.

An exact ROM is successfully utilized to obtain the thermoelastic response of finite instead of infinite unit cell arrays. Furthermore, using the ROM, solid mounting strips adjacent to the array are modelled and their influence on the thermoelastic response is accounted for. A robust optimization formulation combined with a filter domain extension approach enabled the new framework to obtain manufacturing tolerant designs satisfying a minimum length scale for the interior of the unit cell array. Uniform material layers are furthermore successfully enforced to allow fabrication with manufacturing methods inspired by a UAM production process.

Opposed to existing TO frameworks for thermoelastic metamaterials, array size effects are thus accounted for in the new TO framework. For an array size of 2 x 3 unit cells, which is considered in the performed optimization, the difference between the thermoelastic response computed using the commonly used homogenization theory and the exact ROM is larger than 100 %. Only for an array size of 120 x 180 unit cells, the maximum unidirectional thermal expansion computed using both methods differs less than 5 %. The influence of the array size on the thermoelastic response of a unit cell array is thus significant. The commonly used homogenization method ignores these size effects. Using the exact ROM, the size effects are however considered, resulting in the optimization of a realistic thermoelastic response for finite unit cell arrays.

A sample of the optimized design, obtained through only limited post-processing, has been fabricated successfully with only minor discrepancies. Experiments have validated the numerical predictions and have shown that a manufacturable and functional finite thermoelastic metamaterial is obtained, with a unidirectional thermal expansion of $(-4 \pm 8)\,\mu\text{m}/(\text{m}^\circ\text{C})$. It is thus concluded, that the proposed design approach is able to generate performant and realizable thermoelastic metamaterial structures.

REFERENCES

[1] Erik Andreassen, J. J. Sondergaard, O. Sigmund, and T. J. Juel. *Optimal design of porous materials*. Ph.d. dissertation, Department of Mechanical Engineering, DTU, Lyngby, 2015.

[2] A. Bensoussan, J. L. Lions, and G. Papanicolaou. *Asymptotic Analysis for Periodic Structures*. North-Holland Publishing Company, Amsterdam, 1978.

[3] Bing Chung Chen, Emílio C.N. Silva, and Noboru Kikuchi. Advances in computational design and optimization with application to MEMS. *International Journal for Numerical Methods in Engineering*, 52(1-2):23–62, 2001.

[4] Robert J. Guyan. Reduction of stiffness and mass matrices. *AIAA Journal*, 3(2):380, 1965.

[5] Masayuki Hirota and Yoshihiro Kanno. Optimal design of periodic frame structures with negative thermal expansion via mixed integer programming. *Optimization and Engineering*, 16(4):767–809, 2015.

[6] R. K. Oruganti, A. K. Ghosh, and J. Mazumder. Thermal expansion behavior in fabricated cellular structures. *Materials Science and Engineering A*, 371(1-2):24–34, 2004.

[7] Ethan M. Parsons. Lightweight cellular metal composites with zero and tunable thermal expansion enabled by ultrasonic additive manufacturing: Modeling, manufacturing, and testing. *Composite Structures*, 223:110656, 2019.

[8] J. Qi and J. W. Halloran. Negative thermal expansion artificial material from iron-nickel alloys by oxide co-extrusion with reductive sintering. *Journal of Materials Science*, 39(13):4113–4118, 2004.

[9] O. Sigmund and S. Torquato. Design of materials with extreme thermal expansion using a three-phase topology optimization method. *Journal of the Mechanics and Physics of Solids*, 45(6):1037–1067, 1997.

[10] Akihiro Takezawa and Makoto Kobashi. Design methodology for porous composites with tunable thermal expansion produced by multi-material topology optimization and additive manufacturing. *Composites Part B*, 131:21–29, 2017.

[11] Akihiro Takezawa, Makoto Kobashi, and Mitsuru Kitamura. Porous composite with negative thermal expansion obtained by photopolymer additive manufacturing. *APL Materials*, 3(7), 2015.

[12] Fengwen Wang, Boyan Stefanov Lazarov, and Ole Sigmund. On projection methods, convergence and robust formulations in topology optimization. *Structural and Multidisciplinary Optimization*, 43(6):767–784, 2011.

[13] Yan Xie, Xu Pei, and Jingjun Yu. Double-layer sandwich annulus with ultra-low thermal expansion. *Composite Structures*, 203:709–717, 2018.